Journal of the European Ceramic Society 21 (2001) 1195–1204

www.elsevier.com/locate/jeurceramsoc

Mechanical behavior of cordierite and cordierite–mullite materials evaluated by indentation techniques

M.A. Camerucci [a,*], G. Urretavizcaya [b], A.L. Cavalieri [a]

[a] *Instituto de Investigaciones en Ciencia y Tecnología de Materiales, (INTEMA), Universidad Nacional de Mar del Plata-CONICET, Juan B. Justo 4302 (7600) Mar del Plata, Argentina*

[b] *Centro Atómico Bariloche, Bustillo km 9,5 (8400) Bariloche, Argentina*

Received 26 August 2000; received in revised form 15 November 2000; accepted 20 November 2000

Abstract

Commercially available cordierite and mullite powders were used to obtain cordierite and composite materials with mullite content up to 65 wt.% by attrition milling, uniaxial pressing and sintering. Cordierite powders were the coarse, medium and fine single granulometric fractions and the binary mixtures of them with 30, 50 and 70 wt.% of the smaller component. Mullite powder employed in composites was the 7 h-attrition milled one. The Vickers hardness (H_V) and fracture toughness (K_{IC}) were measured by Vickers indentation techniques. The Knoop hardness (H_K) and Young's modulus (E_K) were estimated by Knoop indentation method. Fracture surfaces of sintered materials were analyzed using a scanning electron microscope (SEM). The indentation load to determinate the fracture parameters was previously determined. The influence of the porosity, increasing mullite and glassy phase contents and grain size on the mechanical parameters were analyzed and a fracture mechanism was proposed.

Keywords: Cordierite; Hardness; Indentation methods; Mechanical properties; Mullite

1. Introduction

Cordierite ($2A1_2O_3.5SiO_2.2MgO$) and mullite ($3A1_2O_3.2SiO_2$) represent technically important ceramics which are applicable in a variety of areas.

The low dielectric constant, high resistivity, elevated thermal and chemical stability and very low coefficient of thermal expansion of cordierite are adequate properties that together with low processing costs characterize a potentially available material to be used as substrate in replacement of the alumina, traditionally employed in the electronic industry.[1–3] However, cordierite has the disadvantage of its inferior mechanical properties.[4] Moreover, cordierite ceramics are difficult to sinter without any sintering aids because the sintering must be accomplished by a liquid-phase process. Unfortunately, the properties of cordierite are degraded by sintering aids.[5,6]

Mullite is used as structural material due to its excellent mechanical properties even at high temperatures and is also considered a suitable material for electronic packages.[7,8] By formulating cordierite–mullite composites it is possible to improve the mechanical behavior. However, the presence of mullite aggravates even more the sintering of the cordierite materials.

There have been several studies related to the use of a simple technique such as the indentation method to obtain mechanical parameters such as hardness, Young's modulus and fracture toughness.

The objective of this paper is to evaluate the influence of the additions of mullite on the mechanical behavior of cordierite-based composite materials.

2. Experimental procedure

2.1. Starting powders

Commercially available powders of cordierite (CORCR Baikowski, France) and mullite (MULCR Baikowski, France) were used. Their mean particle sizes were measured using a Coulter LS 130 analyzer with Dolapix PC33 as deflocculant. The values obtained were 1.82 μm for the cordierite powder and 2.35 μm for the mullite powder.

* Corrresponding author.
E-mail address: andcamer@fi.mdp.edu.ar (M.A. Camerucci).

0955-2219/01/$ - see front matter
PII: S0955-2219(00)00334-4

The values of the specific surface areas (BET) measured in a Monosorb Quantachrome equipment were 3.4 and 2.3 m^2/g, respectively. The contents of the elements were determined by wet chemical analysis being the impurity level less than 0.17 wt.% for cordierite powder and 0.3 wt.% for mullite powder (Table 1). The real densities (δ_R) of cordierite and mullite powders were determined by kerosene and He picnometry (Multipicnometry, Quantachrome, USA), respectively, the obtained values are $\delta_{Rcordierite} = 2.6 \quad g/cm^3$ and $\delta_{Rmullite} = 3.05 \quad g/cm^3$.

2.2. Preparation of cordierite and cordierite–mullite materials

As-received cordierite and mullite powders were attrition-milled[9] using a mill with a cylindrical stainless-steel chamber coated with Teflon (700 cm^3). The attrition milling was conducted in a constant isopropyl alcohol volume (360 ml) using alumina balls as grinding media (1–2 mm in diameter). The ball to powder weight ratio employed was 0.2 (0.33 v/v).

Several milling times were selected to prepare the cordierite particle size distributions in order to obtain the single fractions and their binary mixtures. The starting powder (with its initial granulometry) and the powders milled at 1045 rpm during 8 and 32 h were chosen as coarse C, medium M ($D_{50} = 0.9$ μm; $S_S = 6.5$ m^2/g) and fine F ($D_{50} = 0.45$ μm; $S_S = 11.2$ m^2/g) single fractions. The binary mixtures of them F/C, M/C and F/M were prepared in three ratios: 30/70, 50/50 and 70/30 wt.%.

The composite materials were prepared using mullite powder milled at 880 rpm during 7 h ($D_{50} = 1.3$ μm; $S_S = 6.4$ m^2/g). Two sets of cordierite–mullite mixtures were formulated: one of them by addition of 30 wt.% mullite to the cordierite matrices and the other with different proportions of milled mullite powder (0, 10, 30 and 65 wt.%) into the F/C 50/50 cordierite matrix. These samples will hereafter be referred to as cordierite matrix-30M and M_0, M_{10}, M_{30} and M_{65}, respectively.

The preparation of the mixtures was performed by homogenizing of the powders in the attrition mill using alumina media in isopropyl alcohol at 1045 rpm for 10 min; drying in an electrical furnace at 80°C for 24 h and sieving through 37 mesh.

Table 1
As-received cordierite and mullite powders wet chemical analysis

Chemical analysis (wt.%)	Cordierite	Mullite
W.L.	0.004	0.13
Al_2O_3	36.9	72.7
SiO_2	49.4	27.2
MgO	12.32	0.008
Fe_2O_3	0.03	0.02
TiO_2	0.013	0.01
CaO	0.10	0.07
Na_2O	0.02	0.06
K_2O	0.004	0.003

Pellets (1.2 cm in diameter × 0.3 cm in height) of the resulting cordierite and cordierite–mullite particle mixtures were uniaxially pressed at 20 MPa without binders and sintered in an electrical furnace with $MoSi_2$ heating elements at 1450°C, 2 h using a slow firing schedule.[10] The microstructures of the sintered materials were observed by scanning electron microscopy (SEM) on polished with diamond paste from 6 to 1 μm and thermally etched surfaces. The thermal etching was made at 1400°C, 30 min, with a heating rate of 20°C/min. The average grain size was determined by image analysis (Image-Pro Plus software) on the digitized SEM photographs. The apparent densities of the sintered materials (δ_S) were measured by Archimedes method in distilled water. The relative density percentages (% δ_S/δ_R) were calculated using the real densities (δ_R) of the powders treated at 1450°C, 2 h. The last values were obtained considering the parallel mixing rule. For this calculus, the theoretical densities of the present phases and their amounts were considered. The present phases (cordierite, mullite and glass) were determined by XRD and FTIR after heating at 1450°C and the amounts were obtained by examining the isothermal section at the Al_2O_3.SiO_2.MgO system at this temperature.

2.3. Mechanical parameters

The Vickers indentation method was used to measure the Vickers hardness (H_V) and the fracture toughness (K_{IC}) from the indentation size and radial crack lengths employing a Tukon 300 microhardness tester and a loading time of 15 s. The Knoop hardness (H_K) and the Young's modulus (E_K) were estimated by measuring the diagonals of the Knoop indentation.[11–16] The measurements were done on the surfaces of the sintered samples successively polished with 6, 3 and 1 μm diamond pastes. The error of H was 5%, while the error of K_{IC} and E was 10%.

The Vickers and Knoop hardnesses were determined employing the equations: $H_V = 470$ L/a^2 and $H_K = 14229$ L/d^2, respectively, where L is the indentation load in newtons; a is the Vickers characteristic dimension (semidiagonal) and d is the Knoop longest diagonal, both in micrometers.

Young's modulus was estimated using the following equation:[14] $b'/d' \approx b'/d = b/d\text{-}\alpha H_V/E_K$ where $b/d = 1/7.11$ is the ratio of the diagonal dimensions for the Knoop geometry, b'/d' is the ratio of the residual Knoop indentation impression after loading, $\alpha = 0.45$ is an empirical coefficient,[15] H_V is the Vickers hardness and E_K is the Young's modulus.

Fracture toughness was determined using the equation reported by Miranzo et al.[17] that considers median cracks. The K_{IC} values were obtained by an upper

(E_{max}) and lower (E_{min}) boundaries on the elastic modulus (E), which were calculated according to the empirical equation proposed by Knudsen and Spriggs.[18] This relationship establishes the dependence between the Young's modulus and the porosity $E = E^0[\exp(-bP)]$[19–21] where E^0 is the Young's modulus at zero porosity (elastic modulus of a pore-free material), P is the porosity volume fraction and b is a constant determined by the Poisson's ratio that depends on the shape of the pores and their distribution. In each case, the E^0_{max} and E^0_{min} values used were obtained by assuming both the parallel and the series models, respectively[21] with $E^0_{mullite} = 210$ GPa, $E^0_{cordierite} = 134$ GPa and $E^0_{glass} = 73$ GPa.[22,23]

Fracture surfaces of sintered materials broken in biaxial flexure were analyzed using a scanning electron microscope (SEM).

3. Results and discussion

3.1. Al_2O_3–SiO_2–MgO system

The compositions of the starting and composite materials were located in the isothermal section at 1450°C at the Al_2O_3–SiO_2–MgO system.[24]

For this purpose, just the amounts of silica, alumina and magnesia of the cordierite powder were considered, adding the percentage of CaO to that of MgO. This assumption can be made because of the low level of the impurities and the possibility of the formation of a solid solution between cordierite and calcium up to 4.7 wt.%.[25,26] Moreover, anorthite that is observed beyond this limit, was not identified in this study, supporting the above consideration.

The weight percentages of silica, alumina and magnesia calculated were $SiO_2 = 50\%$, $Al_2O_3 = 37\%$ and MgO = 13% locating the composition of the starting cordierite powder in the crystallization field of mullite, in the cordierite–mullite–glass compatibility triangle close to the cordierite stoichiometric composition ($SiO_2 = 51.4\%$, $Al_2O_3 = 34.8\%$ and MgO = 13.8%). The calculated weight percentages of the phases were 84% cordierite, 10% mullite and 6% glass, the last containing 63% SiO_2, 25% Al_2O_3 and 12% MgO. The phases identified (cordierite and mullite) by XRD and FTIR and the determined real density ($\delta_R = 2.6$ g/cm^3) which resulted higher than the theoretical value support the localization of the composition of the cordierite powder.

For the mullite powder, just the amounts of silica (27.2 wt.%) and alumina (72.8 wt.%) were considered. The alumina content of the commercial mullite powder was higher than that of the stoichiometric composition ($SiO_2 = 28.2$ wt.% and $Al_2O_3 = 71.8$ wt.%). This excess of alumina can be present forming a solid solution with mullite.[27] Mullite and cristobalite as a second phase were identified by XRD and FTIR. Thus, from this result and considering the determined real density value ($\delta_{Rmullite} = 3.05$ g/cm^3), the mullite powder composition was located on the edge of the triangle corresponding to the Al_2O_3–SiO_2 binary system shifted towards the corner of the cristobalite in respect of the localization of the mullite stoichiometric composition.

The compositions of the composites were located within the same cordierite–mullite–glass three-phase region on a line that connects the starting compositions of cordierite and mullite commercial powders. For all the composite materials studied the composition of the glass is the same as that determined for the cordierite material but changing their amounts (Table 2).

It is worthy to note that the amount of cordierite diminishes while the amount of the glass increases when the mullite content is higher.

3.2. Densification

In order to obtain the densification degree of the studied materials, the real densities of the powders treated at 1450°C, 2 h were calculated by the parallel mixing rule ($\delta_{M0} = 2.57$ g/cm^3; $\delta_{M10} = 2.64$ g/cm^3; $\delta_{M30} = 2.7$ g/cm^3; $\delta_{M65} = 2.89$ g/cm^3). The values corresponding to the cordierite and composite with 30 wt.% mullite were confirmed by kerosene picnometry. For calculation the theoretical densities of the cordierite and mullite (δ_{th} cordierite = 2.52 g/cm^3 and δ_{th} mullite = 3.16 g/cm^3) were considered. The density of the present glassy phase (2.51 g/cm^3) was measured by kerosene picnometry of the glass produced by melting of the appropriate constitutents mixture (63% SiO_2, 25% Al_2O_3 and 12% MgO) in a platinum crucible at 1600°C for 2 h, followed by quenching in water. The amounts of the three components were determined by examining the isothermal section at 1450°C. Finally, the relative densities of the sintered composite materials were calculated as the ratio of the apparent densities of the materials measured by water immersion and the real densities of the composites.

The densification degree reached by sintering of the single fractions of cordierite and the composites of them with 30 wt.% mullite increases in the order C < M < F (from 94.16 to 97.27% for cordierite and from 95.56 to 98.15% for cordierite–30 wt.% mullite) in agreement with the increment in the green densities. Regarding the densification degree of the binary mixtures, a simple order was

Table 2
Compositions (wt.%) of the composities calculated at 1450°C

Materials	Cordierite (wt.%)	Mullite (wt.%)	Glass (wt.%)
F/G 50/50–0% M	84	10	6
F/G 50/50–10% M	72	19	9
F/G 50/50–30% M	50	35	15
F/G 50/50–65% M	9	64	27

not obtained; not always the best green densities produced higher final densities. The obtained densities (98.05% for cordierite and 98.52 for cordierite–30 wt.% mullite) were only slightly greater or similar to those reached with the materials prepared with the single fractions.

In the present study, it can be seen that as the percentage of mullite increased, the densification degree of the materials showed a no linear increment (M_0 = 95.72%; M_{10} = 96.95%; M_{30} = 98.15%; M_{65} = 97.58%). This result indicates that, in disagreement with reported data,[28,29] mullite doesn't produce an inhibitor effect on the densification of cordierite materials. This fact can be explained considering that a liquid-phase sintering mechanism operates and that the amount of the glassy phase increases with the added mullite content. In all the studied materials, the final grain size was smaller than the initial particle size, this fact strongly supports the assumption that the sintering in presence of a liquid phase occurs almost exclusively through primary and secondary (particle–particle) rearrangements.

3.3. Microstructural analysis

The developed microstructures, so much in the cordierite materials as in the composite materials with mullite content of 30 wt.% were very similar with the exception of that observed in the composite with 65 wt.% of mullite (M_{65}). In Fig. 1, SEM photographs of M_0; M_{30} and M_{65} are shown.

Homogeneous microstructures with mainly equiaxial grains of similar submicronic size (0.3–0.52 μm) and few spherical pores with sizes close to grain sizes were observed and there were no morphological differences to distinguish between the grains of cordierite and mullite. Additionally, a few elongated grains (aspect ratio ≈ 1.9) attributed to mullite were observed. Moreover, the total porosity of the cordierite materials is the highest and corresponds at a lower amount of pores with sizes slightly higher than that observed in the composite materials with 30 wt.% mullite. In these last materials, so much the size as the size distribution of pores are similar.

Significant differences can be observed in the microstructure of the composite materials formulated with 65 wt.% of mullite: a higher amount of elongated grains with large aspect ratio (≈ 3) and few equiaxial ones (0.54 μm) are present. Also, the detected porosity is manifestly higher than that observed in the other cordierite–mullite materials in agreement with its very much smaller relative density.

3.4. Mechanical behavior

3.4.1. Effect of the indentation load

In order to select the indentation load to determinate the fracture parameters (hardness and fracture toughness) the dependence on load was studied using loads ranging from 1 to 40 N. This study was made on the matrix of cordierite F/C 50/50 and the composite M_{30}.

In Fig. 2 the Vickers and Knoop hardnesses as a function of the indentation load for both materials are shown. In both materials, the Vickers and Knoop hardnesses decrease with the increasing load down to a constant value. The reasons of the high dependence of the hardness on the load in the region of low loads have never been satisfactorily explained.[13]

The Vickers hardness (7.6 GPa for M_0 and 8.7 GPa for M_{30}) is essentially constant above 2 kg, while the Knoop hardness (6.6 GPa for M_0 and 7.2 GPa for M_{30}) achieves a constant value for loads higher than 3 kg. In the cordierite and composite materials, the Vickers hardness is lower than the Knoop hardness for loads inferior to 4 and 1 N, respectively. The contrary occurs beyond these values, resulting the Vickers hardness significantly higher than the value measured with the Knoop indenter: a portion of the energy needed to create the indentation is dissipated by the crack formation that mainly occurs during the loading.[13]

Numerous but very similar equations have been proposed[13] to calculate the fracture toughness from the Vickers indentation data. In order to select the equation to be used, one factor to take into account is the type of crack system: the median crack system which consists of two half-penny-shaped cracks and the Palmqvist crack system where four semielliptical cracks are formed.

The two crack systems can be distinguished by the relationships between the load (L) and the crack length (c for

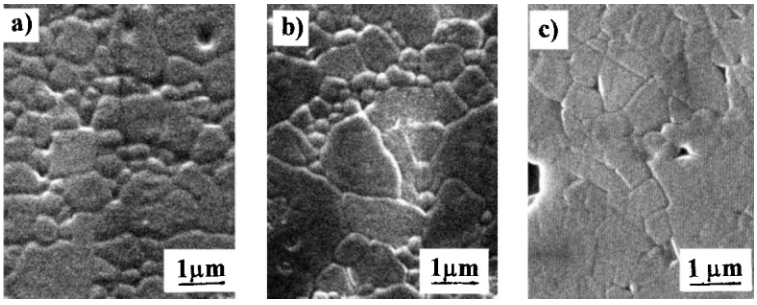

Fig. 1. SEM micrographs of (a) M_0, (b) M_{30} and (c) M_{65} materials sintered at 1450°C, 2 h and thermally etched at 1400°C, 30 min.

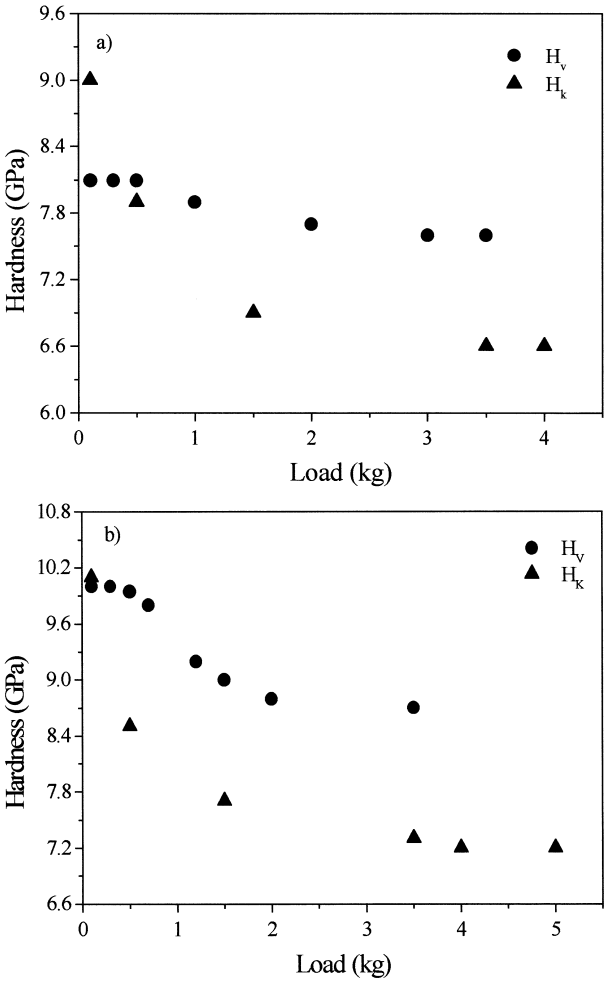

Fig. 2. Vickers and Knoop hardnesses of (a) cordierite and (b) cordierite–30 wt.% mullite as a function of the indentation load.

median cracks or $l = c\text{-}a$ for Palmqvist cracks). The expressions used are: $c = AL^{2/3}$ and $l = BL$, respectively, where A and B are constants that include E, H and K_{IC}.[13]

For many ceramic materials with low fracture toughness values, apparently only the median crack system develops during Vickers indentation.

The type of crack developed in the cordierite and cordierite–30 wt.% mullite was analyzed using the relationships given above. For the cordierite material, the experimental results are better fitted by the median crack approach. However, for the composite material, it results very difficult to differentiate between the two types of crack system. Additionally, in order to observe by SEM the cracks profiles induced around the indentation zone, the specimens were broken under biaxial flexure (Fig. 3). As much at high load (4.5 kg) as at low load indentation (500 g), just median cracks (stable fracture zone) and the fast fracture zone were hardly identified. Moreover, at high load the formation of lateral cracks as well as one zone immediately below the indenter where the material is highly compressed were observed, this can be associated to that designated

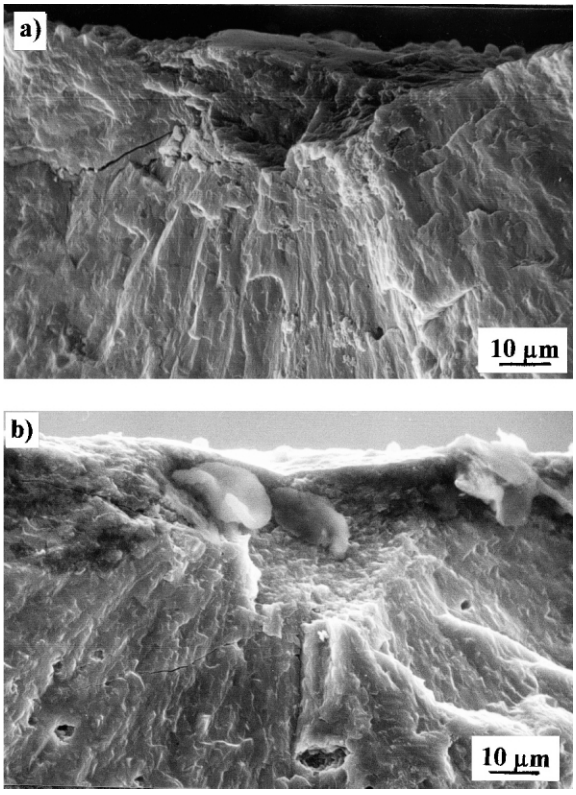

Fig. 3. Fracture surfaces of (a) cordierite and (b) cordierite–30 wt.% mullite.

'core'.[14] The fractographic sizes of the indentation impressions are close to those measured. According to this result, the relation proposed by Miranzo et al.[17] that assumes a median crack system was employed to calculate the fracture toughness.

In Fig. 4 the variation of the fracture toughness values with the indentation load for both materials is shown.

In both materials, the K_{IC} values increase as indentation load increases to attain a constant value, being higher the values calculated with E in parallel than those with E in series. The fracture toughness of cordierite material tends at constant values ($K_{IC} = 1.79$ and 1.74 MPa $m^{1/2}$ for E in parallel or in series, respectively) above 2 kg, while these values are slightly higher ($K_{IC} = 1.97$ and 1.78 MPa $m^{1/2}$) for the composite at loads higher than 3 kg. The addition of 30 wt.% of mullite always produces an increment in the toughness.

Taking into account the load for which the hardness and fracture toughness resulted constant, the Vickers and Knoop indentations tests to determine the effects of porosity and mullite content were performed using loads of 3.5 and 4 kg, respectively.

3.4.2. Effect of the porosity

The influence of the porosity ($\%P = 100 - \% \ \delta_S/\delta_R$) of the cordierite and cordierite–30 wt.% mullite materials on the E_K, H_V and K_{IC} was studied.

Fig. 5 shows the dependence of the Young's modulus estimated by the Knoop indentation on the porosity of cordierite and cordierite–30 wt.% mullite materials. In both materials, the Young's modulus decreases with the increasing porosity due to the contribution of the pores with a null value of E. In the whole porosity range, it was obtained a lower variation of the Young's modulus for the cordierite materials (123.6–116.1 GPa) in respect of that obtained for the composites (136.6–122 GPa).

The experimental values were fitted employing the empirical equation proposed by Knudsen and Sprigss.[18] Another expression, such as that reported by Mackenzie, $E = E^0(1\text{-}bP)$, where E^0 is the Young's modulus at zero porosity and b is a constant that depends on the porosity type, could be used due to the narrow porosity range ($< 5\%$) analyzed.[20,30] However, using the last correlation the value of the constant obtained ($b = 0.0035$) results much lower than that corresponding to spherical close pores ($b = 1.9$) as the observed in these materials.

The b values for the studied materials were calculated from the slope of the lines ln E_k vs P. The value determined for cordierite materials ($b = 3$) is in agreement with that reported by Mussler et al.[22] while a higher value ($b = 4$) was determined for the cordierite–30 wt.% mullite material. However, the fracture toughness values for both cordierite and composite materials were calculated using $b = 3$ because of the values for composites resulted only 1–2% lower by employing $b = 4$.

In Fig. 6 the dependence of the Vickers hardness on the porosity for the cordierite and cordierite–30 wt.% mullite is shown. For both materials, the hardness diminishes with the increasing porosity due to the larger contribution of the plastic deformation component. The hardness changes with the porosity from 8.1 to 6.4 GPa for cordierite materials (porosity range: 2–7.5%) and from 9 to 7.4 GPa for the composite materials (porosity range: 1.5–5%).

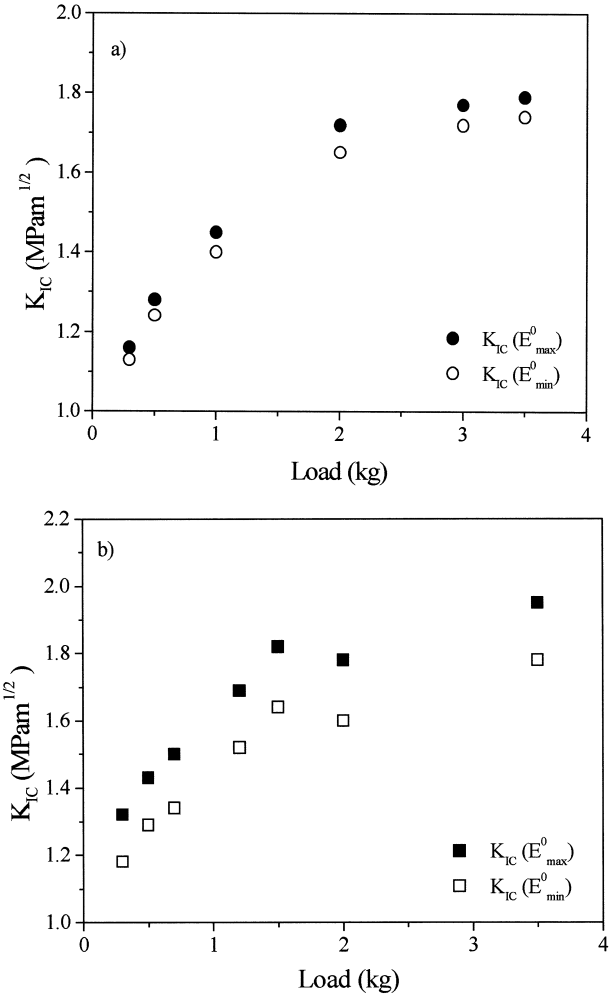

Fig. 4. Fracture toughness (K_{IC}) (Young's modulus in parallel and series) of (a) cordierite and (b) cordierite–30 wt.% mullite vs indentation load.

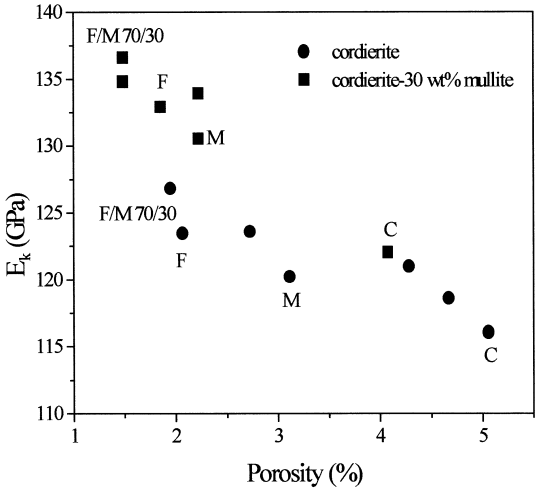

Fig. 5. Dependence of the Young's modulus (E_K) on the porosity of cordierite and cordierite–30 wt.% mullite.

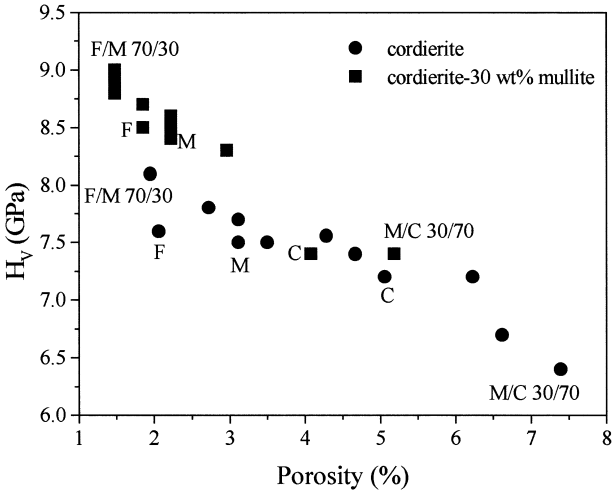

Fig. 6. Vickers hardness (H_V) vs porosity for cordierite and cordierite–30 wt.% mullite.

The hardness values decrease with the increase of the porosity in the cordierite matrices *C*, *M* and *F* as well as in composites with 30 wt.% of mullite ($H_VF > H_VM > H_VC$).

The upper and lower values of hardness for both types of materials correspond to *F*/*M* 70/30 (8.1 and 9.6 GPa) and *M*/*C* 30/70 (6.4 and 7.4 GPa) cordierite matrices with the higher and lower amounts of finer fraction, respectively.

The experimental data were fitted assuming an exponential expression that relates the hardness and the porosity: $H = H^0[(\exp\text{-}cP)]$[22,31] where H^0 is the hardness at zero porosity and *c* is a constant. The following *c* values for both systems were calculated: $c = 3.3$ for cordierite materials and $c = 5.4$ for composites with 30 wt.% of mullite. It must be noted that these values are different than those reported by Mussler et al.[22] ($c = 6$) for similar systems.

In respect of the variation of the fracture toughness with the porosity for the studied materials, a similar behavior determined for hardness was observed (Fig. 7). It can be attributed to the effect of the cracks along the grain boundaries in respect of the pores as stress concentrators because of the pore and grain sizes are similar. K_{IC} decreases with the porosity increasing from 1.90 to 1.67 MPa $m^{1/2}$ for the cordierite materials and from 2.03 to 1.83 MPa $m^{1/2}$ for cordierite–30 wt.% mullite materials.

As in the case of the hardness, it was observed that in both curves the limit values are the corresponding to the cordierite matrices *F*/*M* 70/30 (1.90 and 2.03) and *M*/*C* 30/70 (1.67 and 1.83) and that the values obtained from the single fractions *C*, *M* and *F* follow the same order in agreement with the porosity increasing of these materials ($K_{IC}C < K_{IC}M < K_{IC}F$).

An exponential function of the form $K_{IC} = K^0_{IC}$ [exp (*tP*)] was assumed by fitting the data resulting $t = 2.0$ and $t = 2.4$ for cordierite and cordierite–30 wt.% mullite, respectively. These values are similar to those reported by Mussler et al. ($t = 3$).[22]

3.4.3. Effect of the increasing mullite content

Such as in the load indentation analysis, the cordierite matrix *F*/*C* 50/50 was used. The dependence on the composition of the Young's modulus *E*, hardnesses Vickers H_V and Knoop H_K and fracture toughness K_{IC} was studied.

In Fig. 8 the experimental values of *E* obtained by the Knoop indentation method (load 4 kg) as a function of the increasing mullite content are shown. By increasing the mullite content up to 30 wt.%, the Young's modulus increases continuously. This can be attributed to the lower porosity (from 4.3 to 1.85%) and higher mullite content, being the last effect stronger than that produced by the increment of the glassy phase. However, the value of *E* decreases by 65 wt.% mullite addition due to the predominant effect of the porosity increment (1.85–2.5).

Young's modulus was extrapolated to zero porosity considering the exponential correction mentioned above and it was compared with the values calculated from the parallel and series mixing rules (Fig. 9). It can be noted that the experimental values are intermediate between the calculated ones. The experimental extrapolated data indicate a linear increment with the composition such as the parallel model in good agreement with published data;[22] the values calculated using the series model are approximately constant in all the range of composition analyzed. By removing the effect of the porosity (phase with *E* lower than that of the cordierite) the Young's modulus continuously enhances, even for 65 wt.% mullite inferring that the diminution due to the glassy phase increment would not be outstanding. These results justify to consider in our system (cordierite–mullite–glass) only the parallel model for the Young's modulus calculus.

The variation of the experimental hardness values by increasing the mullite content is shown in Fig. 10. The extrapolated data to zero porosity, H^0_V and H^0_K, assuming the exponential function are also shown. For

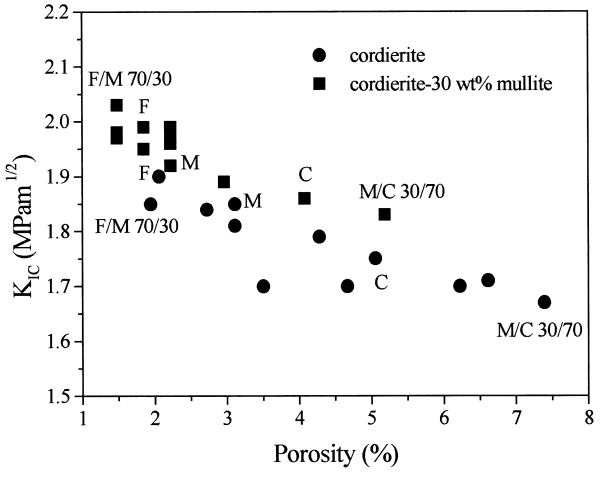

Fig. 7. Fracture toughness (K_{IC}) of cordierite and cordierite–30 wt.% mullite as a function of the porosity.

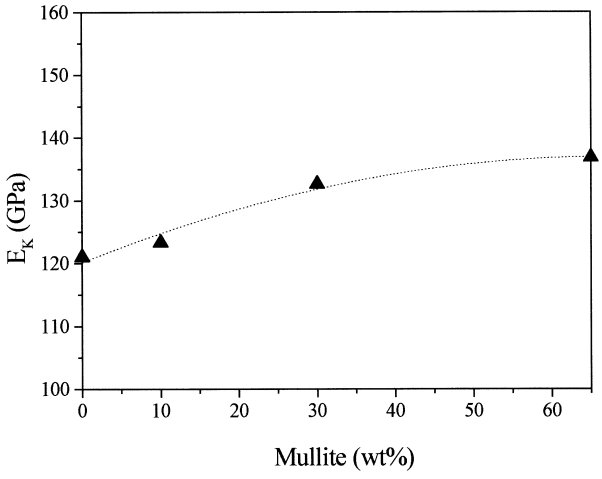

Fig. 8. Young's modulus (E_K) of cordierite–mullite composites.

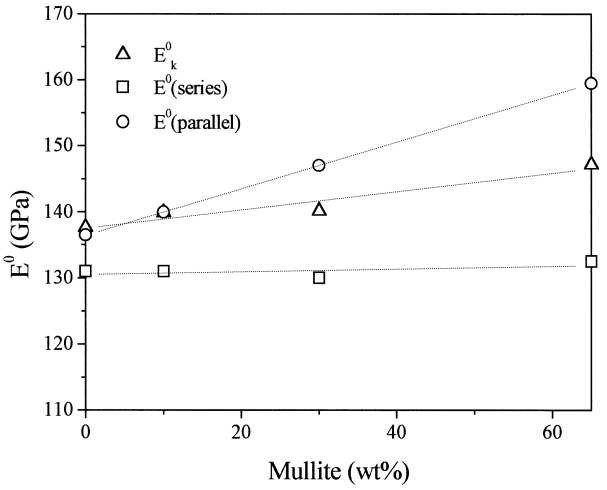

Fig. 9. Young's modulus at zero porosity (E^0_K) and values calculated from the parallel and series mixing rules as a function of the mullite content.

the calculus, c values were obtained by fitting the experimental data as a function of the porosity for cordierite ($c=3.3$) and for cordierite–30 wt.% mullite ($c=5.4$) and were taken from the literature[22] for cordierite–65 wt.% mullite ($c=6$) for similar mullite contents. By increasing the mullite content up to 30 wt.%, Vickers and Knoop hardnesses increased following a similar behavior from 7.6 to 8.9 and from 6.6 to 7.7 GPa, respectively; diminishing the increase rate beyond 30 wt.% mullite. In order to explain these results, it was taken into account the effect of increasing amounts of glass and diminution of the porosity as the mullite content increase, being mullite a phase with higher hardness than cordierite. Up to 30 wt.% mullite, so much the lower porosity as the increasing amount of mullite contribute to increase the hardness, effects that can be prevailing on the deleterious effect of higher glass content. Whereas, for mullite contents between 30 and 65 wt.%, the higher porosity and the glass content in the composites with a greater amount of mullite produce an opposite effect than that caused by increasing the mullite content. For hardnesses at zero porosity, an enhancement of the values as a function of higher mullite and glassy phase contents was observed in the whole studied ranges of composition (from $H_V=$ 8.8 to 9.9 GPa and from $H_K=7.6$ to 8.9 GPa). However, the effects of both phases could not be separated for its analysis.

In respect of the variation of the fracture toughness with the mullite content, the values obtained using the Young's modulus calculated by the Knudsen and Sprigss relationship K_{IC} and the values calculated employing the Young's modulus estimated from Knoop measurements K_{IC} (K) were drawn in Fig. 11. In both cases, by increasing mullite content up to 30 wt.%, an enhance of the values (from $K_{IC}=1.79$ to 1.95 MPa m$^{1/2}$ and from K_{IC} (K) $=1.78$ to 1.99 MPa m$^{1/2}$) was observed. A similar behavior to that obtained for hardness was observed becoming linear by removing the effect of the porosity, $K^0_{IC}K_{IC}[\exp(tP)]$[22] (from $K^0_{IC}=1.95$ to 2.04 MPa m$^{1/2}$ and K^0_{IC} (K) $=1.94$ to 2.08 MPa m$^{1/2}$). The observed facts could not be explained.

3.4.4. Effect of the grain size

There are not many studies and numerous discrepancies with respect to the E, H and K_{IC} dependence on the grain size in ceramic materials.[32–35] In the present study, Young's modulus, Vickers hardness and fracture toughness values extrapolated to zero porosity as a function of grain size for cordierite and cordierite–30 wt.% mullite materials have been analyzed.

The values of the studied fracture parameters resulted independent of grain size in agreement with some data reported.[33] However, it must be noted that the error of the indentation method is high, that the grain size

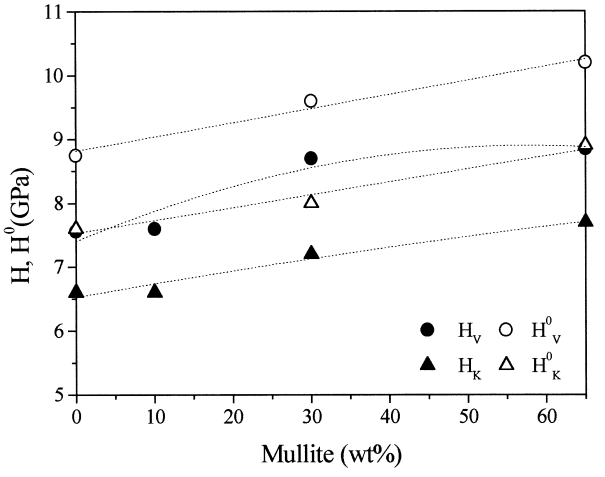

Fig. 10. Hardness values (H_V and H_K) and values at zero porosity (H^0_V and H^0_K) as a function of the mullite content.

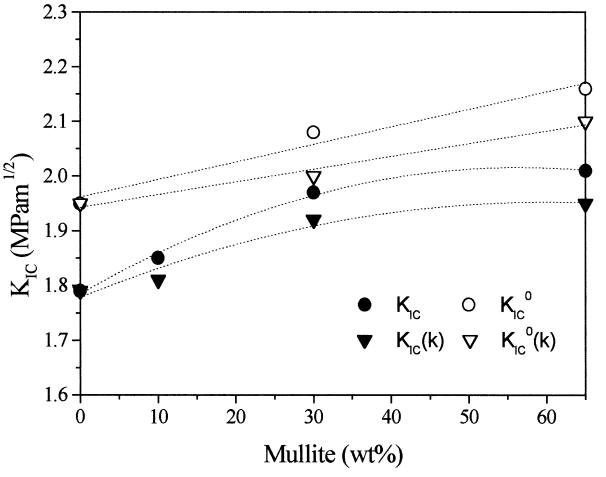

Fig. 11. Fracture toughness [K_{IC} and K_{IC} (K)] and values at zero porosity [K^0_{IC} and K^0_{IC} (K)] as a function of the mullite content.

Table 3
Young's modulus (E_K^0), Vickers hardness (H_V^0), fracture toughness (K_{IC}^0) and mean grain size of cordierite and cordierite–30 wt.% mullite materials

Materials	Mean grain size (μm)	E_K^0 (GPa)[a]	H_V^0 (GPa)[a]	K_{IC}^0 (MPa $m^{1/2}$)
Cordierite	0.30–0.46	132.8	8.6	1.94
Cordierite–30% M	0.45–0.52	140.5	9.6	2.05

[a] Average values in the determined mean grain size range.

developed in all the sintered cordierite and composite materials resulted extremely small and the variation range was very narrow to discard any influence of the grain size on the mechanical parameters. In Table 3 the ranges of the values for cordierite and cordierite–30 wt.% mullite (single fractions and binary mixtures) are reported.

3.5. Fracture mechanism

In Fig. 12, SEM microphotographs of the impression and radial cracks obtained by Vickers indentations of the cordierite and composites with 30 and 65 wt.% of mullite contents are given.

In all the series, the cracks initiate from the corners of the impression, and neither lateral cracks nor spalling were observed. The crack paths were rather tortuous and the fracture surfaces were irregular without branching. In cordierite–65 wt.% mullite, a best definition of the plastically deformed area is observed. This fact was related with the higher proportion of the glassy phase present in this sample.

It results very difficult to identify (Fig. 3) the fracture mode. This is inherent of an intergranular failure whose characteristic fracture are hidden by the microstructure. The increase of the intergranular fracture is related with finer grain size and more regular shapes. Moreover, the defects (impurities and porosity on grain boundaries) introduced during the synthesis of very fine powders, produce intergranular failure, independently of the grain size.[36] Because of the very fine and mainly equiaxiall grains developed in the studied materials and the powder processing and also taking into account the microscopic observations, it is proposed that occurs intergranular failure. The transgranular fracture, that is the fracture mode prevailing in coarse grain materials, can be produced in fine polycrystalline materials due to residual stresses and microcracking by anisotropy in the thermal expansion coefficient. Some toughening mechanism as crack bowing and/or crack deflection operate in intergranular fracture in fine-grained materials in similar systems[37–39] explaining the observed increment in K_{IC} with increasing mullite content. In addition to crack bowing/deflection mechanisms another mechanism due to transgranular fracture operating simultaneously cannot be discarded.

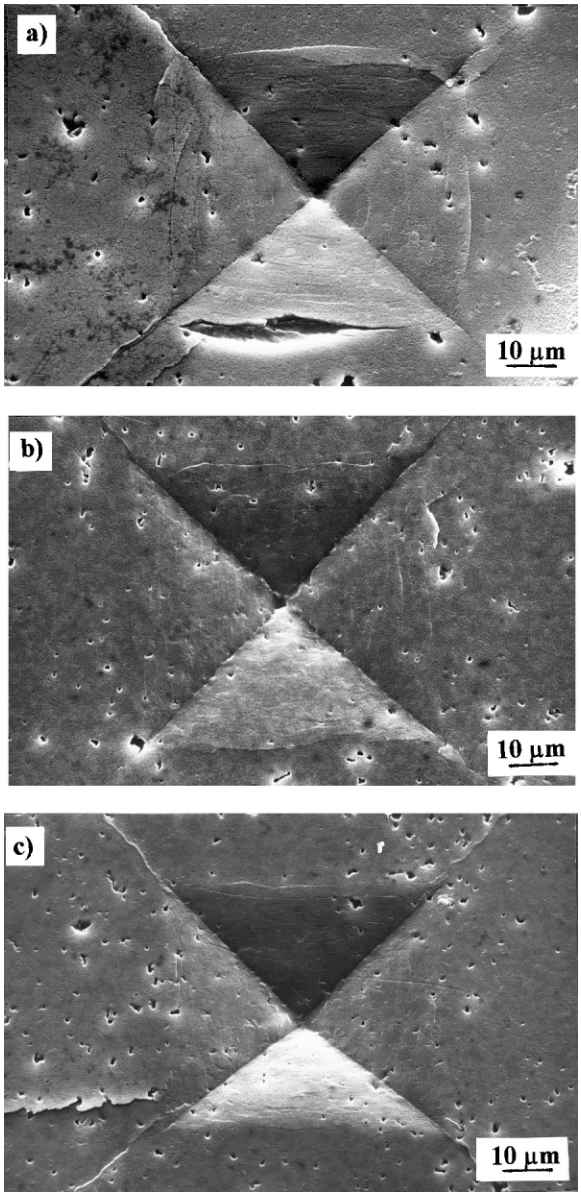

Fig 12. Vickers impressions and radial cracks in (a) M_0, (b) M_{30} and (c) M_{65}.

So, an intergranular fracture with contribution of transgranular can be assumed so much by cordierite and composites materials. The contribution of transgranular fracture is expected to be higher in the sample with 65 wt.% mullite in which there are more elongated grains of mullite besides the equiaxiall grains and with higher size than in the cordierite material.

References

1. Tummala, R. R., Ceramic and glass-ceramic packaging in the 1990s. *J. Am. Ceram. Soc.*, 1991, **74**(5), 895–908.
2. Subramanian, M. A., Corbin, D. R. and Chowdhry, U., Better ceramic substrates through zeolites. *Bull. Mater. Science*, 1993, **16**(6), 665–678.

3. Knickerbocker, S. H., Kumar, A. H. and Herron, L. W., Cordierite glass-ceramics for multilayer ceramic packaging. *Am. Ceram. Soc. Bull.*, 1993, **72**(1), 90–95.
4. Suzuki, H., Ota, K. and Saito, H., Mechanical properties of alkoxy-derived cordierite ceramics. *J. Mater. Sci.*, 1988, **23**, 1534–1538.
5. Awano, M., Takagi, H. and Kuwahara, Y., Grinding effects on synthesis and sintering of cordierite. *J. Am. Ceram. Soc.*, 1992, **75**(9), 2535–2540.
6. Gopi Chandran, R. and Patil, K. C., Combustion synthesis, characterisation, sintering and microstructure of cordierite. *J. Br. Ceram. Trans.*, 1993, **92**(6), 239–245.
7. Kumazawa, T., Otha, S., Kansaki, S. and Tabata, H., Influence of powder characterisitcs on microstructure and mechanical properties of mullite ceramics. *Ceramic Transactions*, 1990, **6**, 401–412.
8. Aksay, I. A., Mullite for structural, electronic and optical applications. *J. Am. Ceram. Soc.*, 1991, **74**(10), 2343–2358.
9. Camerucci, M. A. and Cavalieri, A. L., Process parameters in attrition milling of cordierite powders. *J. Mater. Synthesis and Processing*, 1998, **6**(2), 117–123.
10. Camerucci, M. A., *Desarrollo y Evaluación de Materiales Cerámicos de Cordierita y Cordieritamullita*. PhD thesis, Universidad Nacional de Mar del Plata, 1999.
11. Lawn, B. R. and Marshall, D. B., Hardness, toughness and brittleness: an indentation analysis. *J. Am. Ceram. Soc.*, 1979, **62**(7–8), 347–350.
12. Liang, K. M., Orange, G. and Fantozzi, G., Evaluation by indentation of fracture toughness of ceramic materials. *Mater. Sci.*, 1990, **25**, 207–214.
13. Li, Z., Ghosh, A., Kobayashi, A. S. and Bradt, R. C., Indentation fracture toughness of sintered silicon carbide in the Palmqvist crack regime. *J. Am. Ceram. Soc.*, 1989, **72**(6), 904–911.
14. Lawn, B. and Wilshaw, R., Review indentation fracture: principles and applications. *J. Mater. Sci.*, 1975, **10**, 1049–1081.
15. Marshall, D. B., Tatsuo, N. and Evans, A. G., A simple method for determining elastic-modulus-to-hardness ratios using Knoop indentation measurements. *J. Am. Ceram. Soc.*, 1982, C-176.
16. Dietz, M. and Tietz, H. D., Characterization of engineering ceramics by indentation methods. *J. Mater. Sci.*, 1990, **25**, 3731–3738.
17. Miranzo, P. and Moya, J. S., Elastic/plastic indentation in ceramics: a fracture toughness determination method. *Ceramics International*, 1984, **10**(4), 147–152.
18. Knudsen, F. P., Dependence of mechanical strength of brittle polycrystalline specimens on porosity and grain size. *J. Am. Ceram. Soc.*, 1959, **42**(8), 376–387.
19. Passmore, E. M., Spriggs, R. M. and Vasilos, T., Strength-grain size-porosity relations in alumina. *J. Am. Ceram. Soc.*, 1965, **48**(1), 1–7.
20. Dutta, S. K., Mukhopadhyay, A. K. and Chakraborty, D., Assessment of strength by Young's Modulus and porosity: A critical evaluation. *J. Am. Ceram. Soc.*, 1988, **71**(11), 942–947.
21. Kingery, W. D., *Introduction to Ceramics*. John Wiley & Sons, New York, 1960.
22. Mussler, B. H. and Shafer, M. W., Preparation and properties of mullite–cordierite composites. *Ceram. Bulletin*, 1984, **63**(5), 705–710.
23. Mari, E., *Los Vidrios: Propiedades, Tecnologias de Fabricacion y Aplicaciones*. Américalle, Argentina, 1982.
24. Smart, R. M. and Glasser, F. P., The subsolidus phase equilibria and melting temperatures of $MgO–Al_2O_3–SiO_2$. *Ceramics International*, 1981, **7**(3), 90–97.
25. Scardi, P., Sartori, N., Giachello, A., Demaestri, P. P. and Branda, F., Influence of calcium oxide and sodium oxide on the microstructure of cordierite catalyst supports. *Ceramics International*, 1993, **19**, 105–111.
26. Sundar, S., Vespa, V. S. S. and Umarji, A. M., Effect of substitution of Ca on thermal expansion of cordierite ($Mg_2Al_4Si_5O_{18}$). *J. Am. Ceram. Soc.*, 1993, **76**(7), 1873–1876.
27. Cavalieri, A. L., Pena, P. and de Aza, S., Mullita: Naturaleza de la fusión y rango de solución sólida. *Bol. Soc. Esp. Ceram. Vidr.*, 1990, **29**(3), 171–176.
28. Gopi Chandran, R., Patil, K. C. and Chandrappa, G. T., Combustion synthesis, characterization, sintering and microstrucutre of mullite–cordierite composites. *J. Mater. Sci. Lett.*, 1995, **14**, 548–551.
29. Hodge, J. D., Microstructure development in mullite–cordierite ceramics. *J. Am. Ceram. Soc.*, 1989, **72**(7), 1295–1298.
30. Bailey, J. E. and Hill, N. A., The effect of porosity and microstructure on the mechanical properties of ceramics. *Br. Ceram. Soc.*, 1970, **15**, 15–35.
31. Lee, W. E. and Rainforth, W. M., *Ceramic Microstructures: Property Control by Processing*. Chapman & Hall, London, 1994.
32. Ebadzadeh, T. and Lee, W. E., Processing — microstructure-property relations in mullita–cordierite composites. *J. Eur. Ceram. Soc.*, 1998, **18**, 837–848.
33. Höfler, H. J. and Averback, R. S., Grain growth in nanocrystalline TiO_2 and its relation to Vickers hardness and fracture toughness. *Met. et Materialia*, 1990, **24**, 2401–2406.
34. Rice, R. W., Wu, C. C. and Borchelt, F., Hardness-grain-size relations in ceramics. *J. Am. Ceram. Soc.*, 1994, **77**(10), 2539–2553.
35. Krell, A., Load dependence of hardness in sintered submicrometer Al_2O_3 and ZrO_2. *J. Am. Ceram. Soc.*, 1995, **78**(5), 1417–1419.
36. Rice, R. W., Perspective on fractography. *Adv. Ceram.*, 1988, **22**, 3–56.
37. Faber, K. T. and Evans, A. G., Crack deflection processes — I theory. *Acta Metall.*, 1983, **31**(4), 565–576.
38. Green, D. J., Fracture toughness predictions for crack bowing in brittle particulate composites. *J. Am. Ceram. Soc.*, 1983, C-4.
39. Green, D. J., Nicholson, P. S. and Embury, J. D., Fracture of brittle particulate composite. *J. Mater. Sci.*, 1979, **14**, 1657–1661.